Research Square

Preprints are preliminary reports that have not undergone peer review.
They should not be considered conclusive, used to inform clinical practice,
or referenced by the media as validated information.

Finite Element Analysis of Residual Stress in Cu-20Sn-10Ti Alloy Brazed Diamond

Bing Cui

bingcui6688@163.com

Anhui University of Technology

Yongle Dong

Anhui University of Technology

Tao Jiang

Anhui University of Technology

Quanbin Du

Henan Mechanical and Electrical Vocational College

Lei Wang

Henan Mechanical and Electrical Vocational College

Wei Li

Henan Mechanical and Electrical Vocational College

Juan Liu

Anhui University of Technology

Research Article

Keywords: Cu-Sn-Ti filler alloy, brazed diamond, finite element analysis, residual stress, Raman spectroscopy, process parameters

Posted Date: November 3rd, 2026

DOI: https://doi.org/10.21203/rs.3.rs-11189859/v1

License: This work is licensed under a Creative Commons Attribution 4.0 International License.
Read Full License

Finite Element Analysis of Residual Stress in Cu-20Sn-10Ti Alloy Brazed Diamond

— 3D Thermo-Mechanical Simulation via ABAQUS and Raman Spectroscopy Verification —

Bing Cui[a] , Yongle Dong[a] , Tao Jiang[a] , Quanbin Du[b,*] , Lei Wang[b] , Wei Li[b] ,Juan Liu[a]

Abstract

The interfacial thermal stress in brazed diamond tools originates from the mismatch of thermal expansion coefficients among constituent materials; non-coordinated deformation induced by temperature-field variations leads to thermal-stress concentration. Interfacial residual compressive stress can enhance the holding force of the brazing filler on diamond grits, but excessively high interfacial residual stress may induce cracks and reduce the service life of diamond tools. To accurately characterize the interfacial stress distribution, this study takes single-layer diamond brazed with Cu-20Sn-10Ti filler alloy as the research object. A three-dimensional thermo-mechanical coupled finite element model comprising diamond, the Cu-Sn-Ti filler layer and a 45-steel substrate was established using ABAQUS, and the residual-stress distribution under different brazing temperatures (850-1050 °C) and holding times (1-9 min) was systematically simulated. The results show that both brazing temperature and holding time exhibit a nonlinear trend of first decreasing and then increasing. At 950 °C and 7 min the residual stress reaches minimum values of 417.3 MPa and 402.1 MPa (FEM), respectively, or 463 MPa (Raman measurement); 950 °C / 7 min is thus identified as the optimal process window. Raman spectroscopy verifies the reliability of the finite element simulation: the measured and simulated values share the same trend, fully confirming the accuracy of the method. Grinding tests show that, under the 950 °C/7 min process, diamond grits exhibit a moderate micro-fracture ratio, combining good self-sharpening ability with bond strength, and the tool achieves optimal wear resistance. This study provides a scientific basis for the control of residual stress and process optimization of brazed diamond tools.[1]

[1] Corresponding author E-mail addresses: paperduqb@126.com (Q. Du).

Keywords: Cu-Sn-Ti filler alloy; brazed diamond; finite element analysis; residual stress; Raman spectroscopy; process parameters

1 Introduction

Diamond is widely used in the machining of hard and brittle materials such as stone, ceramics, glass, semiconductor wafers and cemented carbides, owing to its ultra-hardness (Vickers hardness above 10000 HV), extremely high thermal conductivity (about 2000 W/(m·K)) and excellent chemical stability [1-3]. However, the full performance of a diamond tool fundamentally depends on a high-quality connection between the diamond grits and the metal matrix. Traditional electroplated and electroless-plated diamond tools rely solely on mechanical interlocking to hold the grits, resulting in low holding strength, small protrusion height and easy shedding, which can no longer satisfy the demands of high-efficiency precision machining [4,5].

Brazed diamond technology involves melting the filler at high temperature to wet the diamond surface; active elements (such as Ti and Cr) in the filler undergo a metallurgical reaction with diamond, forming a carbide transition layer at the interface and thus achieving high-strength chemical bonding between the binder and the diamond [6-8]. Compared with electroplating, brazed diamond tools can achieve a diamond exposure of 70%-80%, with significantly enhanced grit holding force, large chip-holding space and little tendency for chip clogging, giving them higher grinding efficiency and longer service life [9]. In recent years, with the surging demand for precision and ultra-precision grinding in strategic industries such as semiconductors, optical glass and aerospace, brazed diamond tools have become an important support of industrial foundation-strengthening programs [10].

Although the brazing process greatly improves the holding strength of diamond grits, severe thermal-mismatch stress is generated in the interfacial region during brazing and subsequent cooling because of the huge difference in thermal expansion coefficients among diamond, filler alloy and metal matrix (the coefficient of diamond is only about 1×10^{-6} K^{-1}, whereas Cu-based filler is about $14\text{-}18\times10^{-6}$ K^{-1} and 45 steel about 12×10^{-6} K^{-1}) [11,12]. The generation of interfacial residual stress originates from the mismatch of thermal expansion

coefficients among the constituent materials, and the non-coordinated deformation caused by temperature-field changes leads to thermal-stress concentration.

Interfacial residual compressive stress can, to some extent, enhance the holding force of the filler on diamond grits and suppress crack propagation; however, excessively high interfacial residual stress can induce interface cracking and filler-layer delamination, and may even cause large-area fracture and shedding of diamond grits during service, severely shortening the tool life[13,14]. Therefore, accurately analyzing the interfacial stress distribution and revealing the mechanism by which process parameters regulate residual stress are crucial for the process optimization and performance improvement of brazed diamond tools.

In addition, there is the problem of diamond thermal damage (graphitization) during brazing. Diamond is thermodynamically metastable; in the presence of catalysts such as Fe, Ni and Co at high temperature, sp^3 hybrid bonds readily transform into sp^2 structures, which is manifested in Raman spectra by a shift of the 1332 cm^{-1} characteristic peak toward around 1580 cm^{-1}, forming a graphitized layer[15,16]. Graphitization not only weakens the strength of diamond itself but also deteriorates the interfacial bonding, further aggravating the residual-stress problem. Therefore, how to suppress graphitization and reduce residual stress while guaranteeing interfacial bond strength is a core challenge in current brazed-diamond research.

In the study of brazed diamond tools, finite element analysis (FEA) has become the main method for calculating and predicting interfacial residual stress in diamond[17]. Finite element simulation integrates multiple pieces of information—material properties, process parameters and the brazing environment—to accurately resolve the distribution of internal residual stress and the thermal-deformation behavior during brazing. Zhang Fang et al.[18] used ABAQUS to simulate diamond specimens prepared under different brazing processes and measured the interfacial residual stress by Raman spectroscopy. They found that, because of its faster cooling rate, high-frequency induction brazing produced significantly higher residual stress after brazing than vacuum brazing; regarding filler effect, Ni-Cr alloy generated greater residual stress than Ag-Cu alloy. Raman data showed that after vacuum brazing the stress at the top and bottom of diamond was 25 MPa and 230 MPa, respectively, versus 69.5 MPa and 419.5 MPa for high-frequency induction brazing. The simulation results were highly

consistent with the experimental data, fully verifying the accuracy and reliability of the FEA method.

Akbari et al.[19] performed a thermo-mechanical analysis of the residual stress in diamond joints brazed with Cu-Sn-based active filler by combining Raman spectroscopy with finite element simulation; the peak residual stress was concentrated at the edge of the diamond/filler interface and was directly related to thermal-expansion mismatch. Liu Haihan et al.[20] systematically reviewed the application of FEA to brazing residual-stress analysis, pointing out that the degree of model simplification and the accuracy of material parameters are the key factors determining simulation precision. Junyi Li et al.[21] established a three-dimensional model of diamond brazed with Ni-Cr filler, verified the reliability of FEA through experiments and noted that holding time has a significant influence on the interfacial stress distribution.

However, while FEA offers notable advantages in residual-stress prediction, its application to Cu-based alloy/diamond systems still faces key challenges: (i) because the model is oversimplified (e.g., temperature-dependent material properties and the interfacial reaction layer are ignored), calculated results often deviate considerably from experiments; (ii) residual-stress analysis of brazed diamond is generally limited to a single parameter variable, with few reports on the coupled effects of multiple process parameters; (iii) the combination of FEA simulation with experimental verification remains insufficient, especially for the novel Cu-20Sn-10Ti filler system, which has rarely been studied.

To this end, this study takes single-layer diamond brazed with Cu-20Sn-10Ti filler alloy as the research object. Using ABAQUS, a three-dimensional thermo-mechanical coupled finite element model comprising diamond, the Cu-Sn-Ti filler layer and a 45-steel substrate was established, and the distribution and evolution of residual stress under different brazing temperatures (850-1050 °C) and holding times (1-9 min) were systematically simulated. On this basis, a Raman spectrometer was used to experimentally determine the residual stress of the brazed diamond particles; through cross-validation of simulation and experiment, the mechanism by which process parameters regulate residual stress was revealed. Finally, combined with grinding tests and wear-morphology analysis, the intrinsic relationship

between residual stress and tool wear resistance was clarified, providing a scientific basis for the control of residual stress and process optimization of brazed diamond tools.

2 Experimental Materials and Methods

2.1 Experimental materials

In this experiment, 35-mesh diamond grits and a 45-steel substrate were used, and vacuum brazing was carried out with Cu-20Sn-10Ti filler. The diamond grit size was 0.4 mm (equivalent sphere diameter), the filler-layer thickness was 150 μm, and the 45-steel substrate measured 5 mm × 5 mm × 5 mm. The calculated density of the Cu-20Sn-10Ti filler alloy was 8.185 g/cm³ and its Poisson's ratio was 0.3. Diamond had a density of 3.523 g/cm³, elastic modulus of 882 GPa, Poisson's ratio of 0.0691 and thermal conductivity of 1800 W/(m·K). The 45 steel had a density of 7.81 g/cm³ and a Poisson's ratio of 0.3.

2.2 Establishment of the finite element model

Based on the morphology and dimensions of the experimental specimen, a three-dimensional finite element model of the brazed diamond was established in ABAQUS. Given the differences in arrangement, size and mass of the diamond grits in the brazed specimen, and the difficulty of accurately simulating every phenomenon during brazing under current conditions, the following assumptions were made: (1) diamond is an ideal linear-elastic material, whereas the Cu-Sn-Ti filler and 45 steel are ideal elastoplastic models; (2) the materials are homogeneous, isotropic and free of cracks or other defects, conforming to the von Mises yield criterion; (3) because the heating and cooling rates are slow, the temperature field is assumed to vary uniformly.

For meshing, a denser mesh was used at contacts between different materials and in stress-concentration regions, while a relatively coarse mesh was used in non-contact regions. The total number of nodes was 58,894 and the number of elements was 296,205.

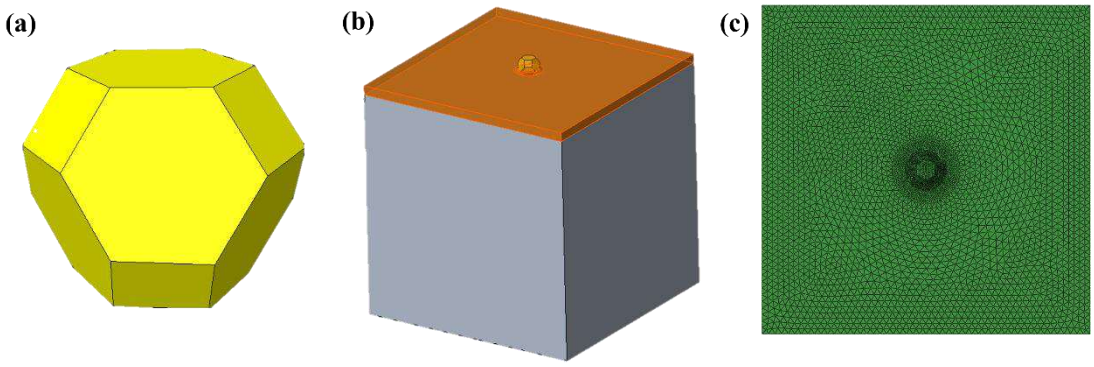


Fig. 1 Finite element model of brazed diamond: (a) diamond model; (b) brazed diamond FE model; (c) meshing.

2.3 Material property settings

The physical parameters of the materials vary with temperature. In this study, temperature-dependent material properties—including elastic modulus, thermal expansion coefficient, specific heat capacity and thermal conductivity—were comprehensively considered.

Table 1 Physical parameters of 45 steel[22]

T, ℃	20	200	400	600	800	1000
E, GPa	200.1	193	172	121	71	20
α, 10^{-6}/k	11.59	12.32	13.71	14.67	12.50	14.40
C, J/kg·℃	472	498	560	700	806	602
k, W/（m·K）	47.68	40.44	36.02	31.98	26.49	24.02

Table 2 Physical parameters of diamond[23]

T, ℃	20	200	400	600	800	1000
α, 10^{-6}/k	1	2.53	3.52	4.07	4.57	5.43

Table 3 Physical parameters of the Cu-Sn-Ti filler[24]

T, ℃	20	200	400	600	800	1000
E, GPa	186	174	162	147	98	/

α, 10^{-6}/k	13.98	15.04	16.15	17.79	20.23	32.56
C, J/kg·℃	368	395	408	422	434	459
K, W/（m·K）	267.96	258.56	240.54	206.94	167.61	52.27

2.4 Load application and boundary conditions

The brazed specimen mainly consists of three parts, with a 0.15 mm Cu-Sn-Ti filler interlayer placed between the diamond and the 45-steel substrate. According to the brazing process, metallurgical bonding occurs among the three parts in the brazing furnace. Therefore, the interlayer was tied to the diamond and to the 45 steel, respectively, to ensure no relative motion and to allow heat transfer between them. To prevent overall rigid-body displacement during temperature changes, a YSYMM constraint was applied to the bottom surface of the 45-steel substrate.

In the actual brazing process, the initial specimen temperatures were set to 850, 900, 950, 1000 and 1050 °C, and the ambient temperature was set to room temperature (25 °C). To avoid excessive residual stress caused by too rapid cooling, the specimen was slowly cooled to room temperature in the brazing furnace before extraction. The finite element method was used to analyze the distribution and variation of internal residual stress in the brazed diamond under different conditions.

2.5 Residual-stress detection method

The Raman characteristic peak of diamond generally appears at 1332 cm^{-1}, and the stress on diamond can be calculated from the Raman peak shift:

$$\sigma_m = |\nu_0 - \nu| / p \quad (1)$$

where ν_0 is the Raman characteristic shift of diamond before brazing, ν is the shift after brazing, and p is generally taken as 2.88. The selected diamond grits had an average particle size of about 425 μm; the focused laser beam was incident from directly above the diamond. The distance h from the upper surface of the diamond to the focal point of the incident laser

was 70 μm, and each diamond was measured 6 times. To ensure accuracy, 10 diamond grits were selected for measurement under each process condition.

2.6 Grinding-performance test method

A high-precision friction and wear tester was used to evaluate the wear resistance of the diamond grinding disk, as shown in Fig. 2.5. An SiC wafer (Φ50 mm diameter, 5 mm thickness) produced by Fuzhou Kunpeng Optoelectronic Technology Co., Ltd. was used as the counterface. During grinding, the applied load was 100 N, the loading time was 1 min, the disk rotation speed was 200 r/min, and each specimen was loaded 5 times. After each loading, the disk was ultrasonically cleaned in anhydrous ethanol for 15 min and air-dried, then the morphology of the worn diamond abrasive was observed with an electron microscope (CX-2KCF). The signal acquisition system of the wear tester recorded the friction coefficient of the diamond disk every second, and an electronic balance was used to measure the material removal of the SiC after wear.

3 Results and Discussion

In the transient heat-transfer analysis of the brazing process, the system temperature field changes significantly with time, and the governing equation is established based on the principle of energy conservation. When the temperature dependence of the material thermophysical properties is considered, the thermal analysis becomes a nonlinear problem that must be solved by an incremental iterative algorithm, usually converged within each time step via the Newton-Raphson method.

In the elastoplastic mechanical analysis, for isotropic materials the von Mises yield criterion is widely used to evaluate the stress state of metallic materials. In the analysis of brazing residual stress, the coupled effect of thermal and mechanical strains must be considered simultaneously, and a constitutive equation incorporating temperature effects must be established. This thermo-mechanical coupling analysis can accurately predict the interfacial residual-stress distribution and its influence on tool performance.

3.1 Effect of brazing temperature on interfacial residual stress

Fig. 2 shows the residual-stress distribution contours and the variation of the maximum stress for brazed diamond specimens at a filler-layer thickness of 0.15 mm under different

brazing temperatures (850, 900, 950, 1000 and 1050 °C). The results show that as the brazing temperature increases from 850 to 950 °C, the residual stress at the bottom of the diamond gradually decreases from 430 MPa to 417.3 MPa; but when the temperature is further raised to 1050 °C, the stress rises back to 444.1 MPa. This trend indicates that 950 °C is the inflection temperature for residual stress.

In the low-temperature range (850 and 900 °C), the increase in temperature improves the wettability of the filler (Cu-20Sn-10Ti) and promotes uniform interfacial bonding, reducing local stress concentration; whereas in the high-temperature range (1000 and 1050 °C), phase transformations within the filler and interfacial reactions (such as excessive TiC-layer formation) reduce the plastic-deformation capacity, and the thermal mismatch intensifies during cooling, leading to higher residual stress. Moreover, the peak residual stress is always concentrated near the diamond/filler interface and decays rapidly with distance, which is directly related to the thermal-expansion mismatch between diamond and filler.

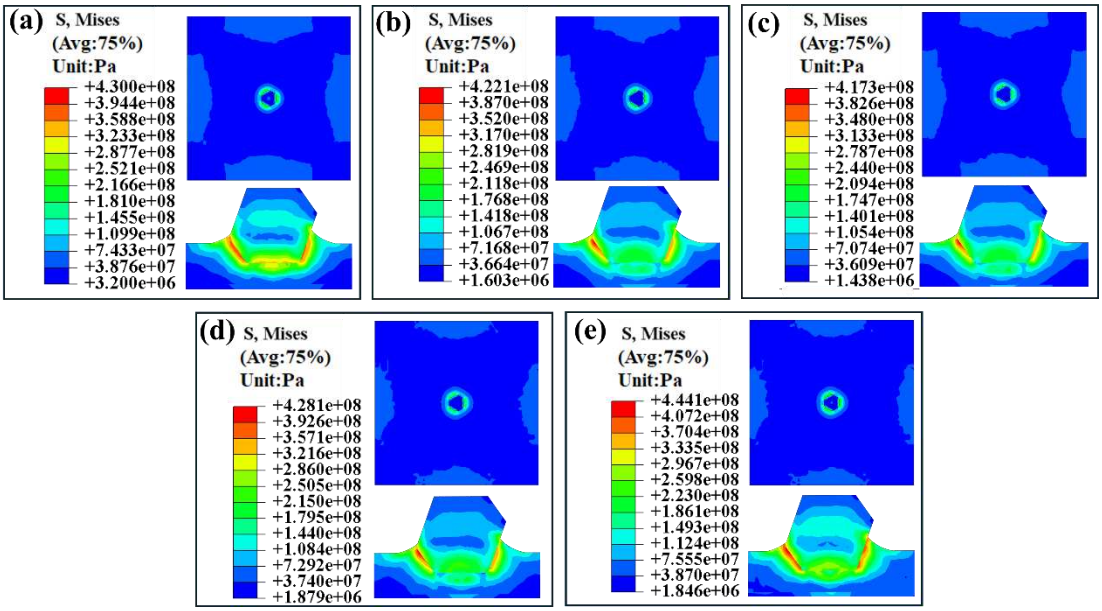


Fig. 2 Residual stress distribution of the specimens under different brazing temperatures: (a) 850 °C; (b) 900 °C; (c) 950 °C; (d) 1000 °C; (e) 1050 °C.

3.2 Effect of holding time on interfacial residual stress

Fig. 3 describes the effect of different holding times (1, 3, 5, 7 and 9 min) on residual stress at a fixed brazing temperature of 950 °C. When the holding time is 1 min, the residual

stress at the bottom of the diamond is 443.8 MPa; as the holding time increases, the residual stress gradually decreases, reaching a minimum of 402.1 MPa at 7 min; when the holding time is further extended to 9 min, the stress rises back to 442.4 MPa.

At too short holding times (1 and 3 min), elemental diffusion (e.g., Ti migration toward the interface) is insufficient and the interfacial TiC layer is discontinuous, leading to inadequate stress release; at too long a holding time (9 min), grain coarsening, interfacial embrittlement (e.g., excessive TiC layer) and diamond graphitization may occur, weakening the plastic-deformation capacity of the filler and ultimately aggravating stress accumulation.

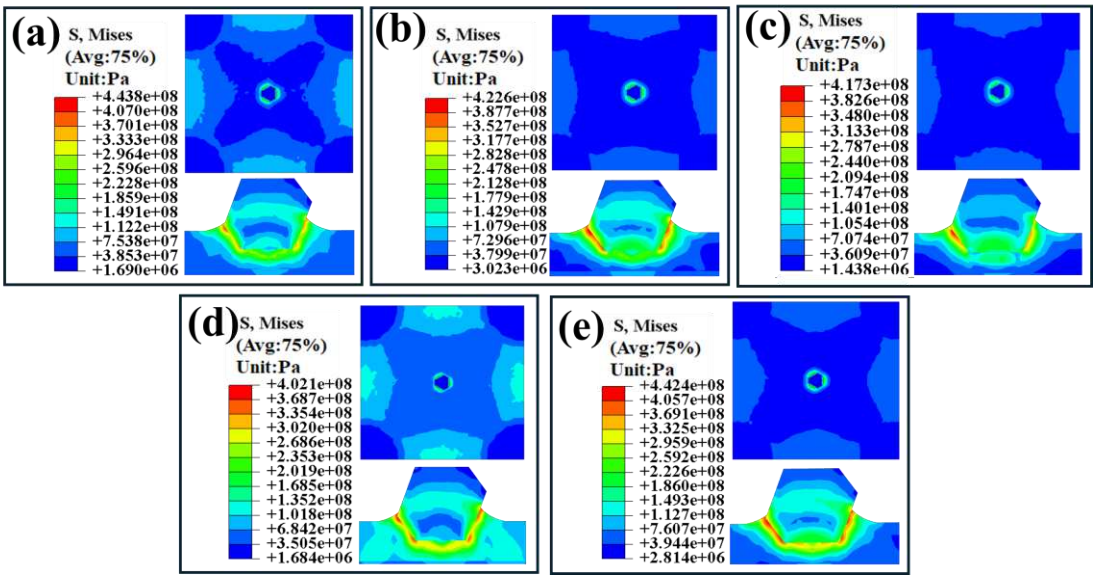


Fig. 3 Residual stress distribution of the specimens under different holding times: (a) 1 min; (b) 3 min; (c) 5 min; (d) 7 min; (e) 9 min.

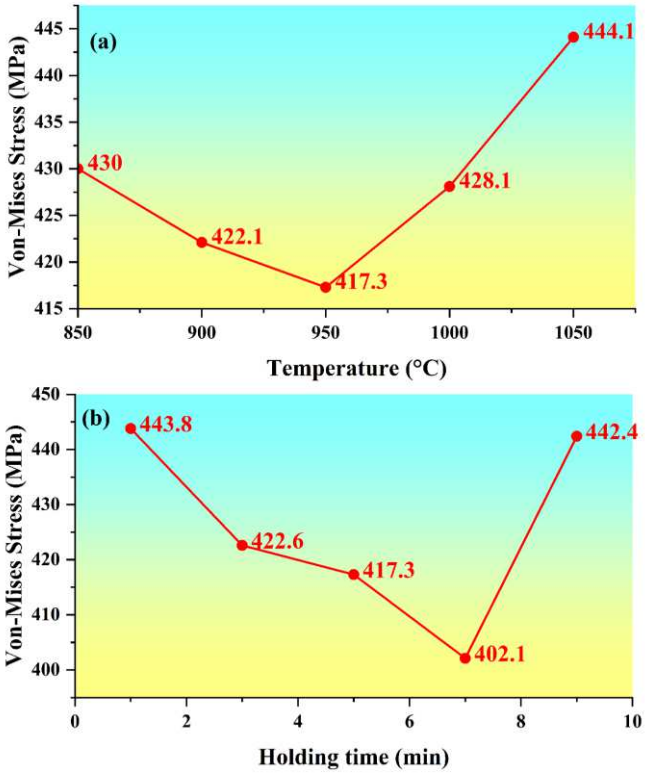


Fig. 4 (a) Residual stress under different brazing temperatures; (b) residual stress under different holding times.

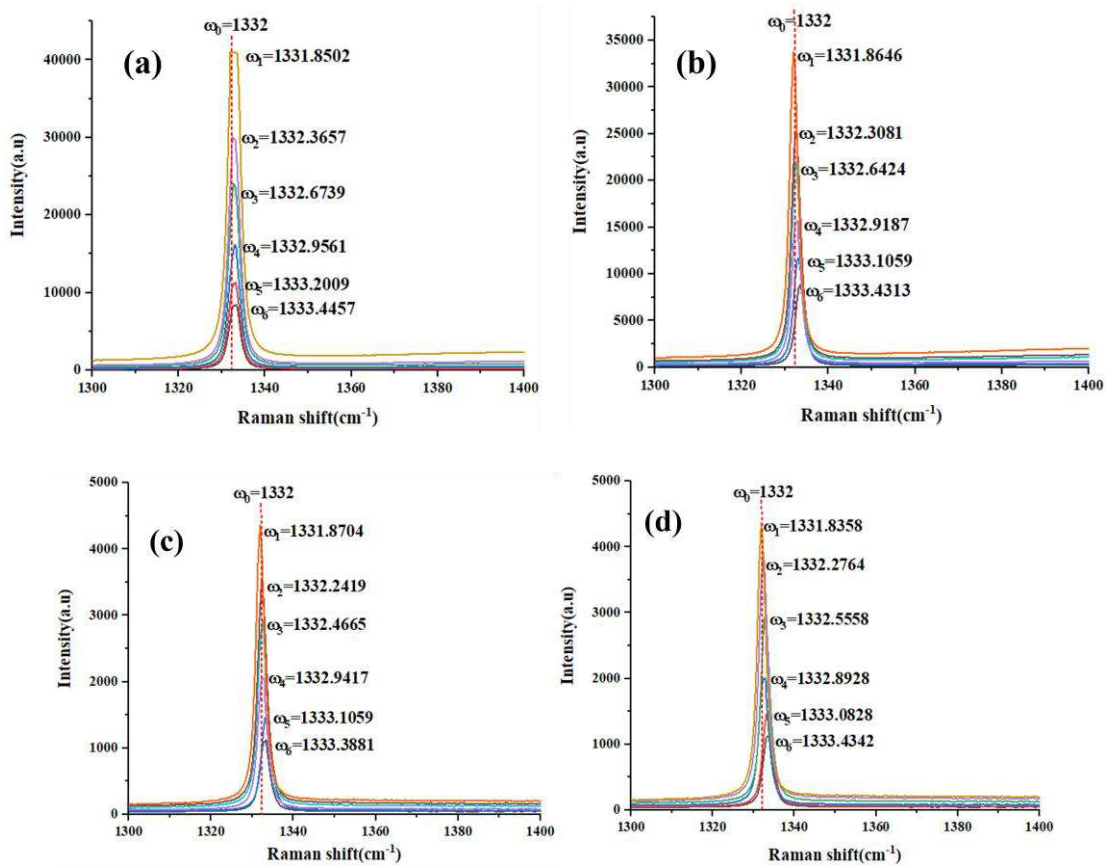
In Fig. 4(a), the minimum stress at 950 °C (417.3 MPa) confirms the optimal balance of the thermo-mechanical coupling effect at this temperature; in Fig. 4(b), the holding time of 7 min corresponds to the minimum stress of 402.1 MPa, indicating that moderate diffusion and interfacial-reaction control are the key to reducing stress. Both curves exhibit a trend of first decreasing and then increasing, which is attributed to the fact that lower temperature or shorter holding time leads to compositional inhomogeneity and low interfacial bonding strength, whereas higher temperature and longer holding time cause defects such as excessive TiC, grain coarsening and diamond graphitization that destroy interfacial stability. Therefore, an intermediate value of the brazing parameters can minimize stress by optimizing material deformation and reaction kinetics.

3.3 Finite element verification by residual-stress detection

The stress in diamond is closely related to the peak position in the Raman scattering spectrum. Under compressive stress, the Raman peak shifts toward higher wavenumber; under tensile stress, it shifts toward lower wavenumber. Fig. 5 shows the Raman peak shift of

diamond particles under different brazing temperatures (850-1050 °C). From the spectral curves, it can be seen that the top of the diamond is under tensile stress at all brazing temperatures, and the tensile stress gradually turns into compressive stress and increases with depth.

Specifically, at 850 and 900 °C the Raman peaks shift significantly toward lower wavenumber; the shifts at the diamond bottom are $\Delta\nu$ = 1.445 and 1.431 cm^{-1}, respectively, corresponding to relatively high compressive stresses at point F (502 and 497 MPa), consistent with the local stress concentration caused by insufficient filler fluidity and poor interfacial wettability at low temperatures. As the temperature rises to 950 °C, the Raman shift is minimized ($\Delta\nu$ = 1.388 cm^{-1}) and the residual stress at point F drops to its lowest value (481 MPa); at this point, optimized filler fluidity and interfacial reaction (uniform TiC-layer formation) effectively alleviate the thermal-expansion mismatch between diamond and filler. However, when the temperature is further raised to 1050 °C, the Raman peak shifts toward higher wavenumber again ($\Delta\nu$ = 1.451 cm^{-1}), and the residual stress at point F rises back to 504 MPa.



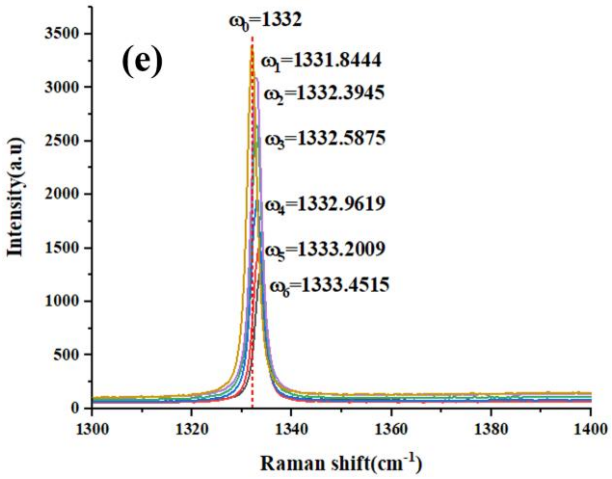
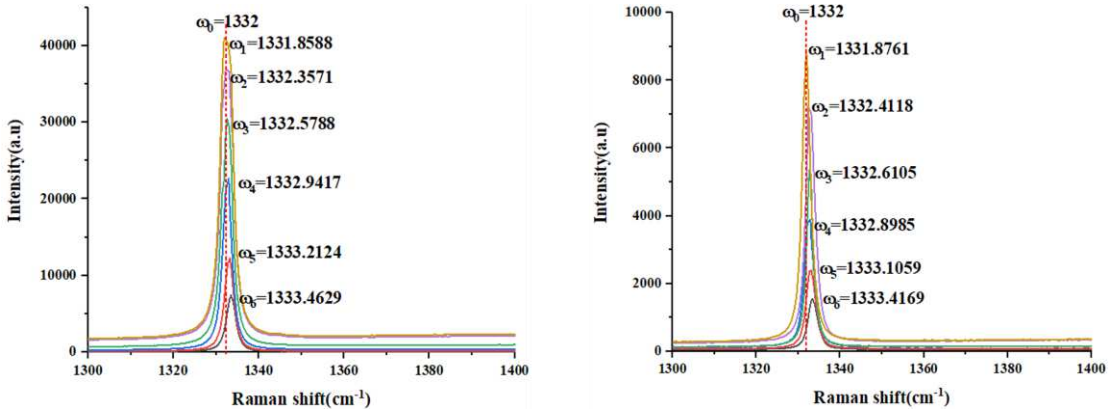


Fig. 5Raman spectra of diamond particles under different brazing temperatures.

Fig. 6 shows the effect of different holding times (1-9 min) on the Raman peak shift of diamond at a fixed brazing temperature of 950 °C. As the holding time increases from 1 to 7 min, the shift of the diamond characteristic peak gradually decreases (from 1333.4629 to 1333.3334 cm^{-1}), indicating a downward trend of the residual stress at the diamond bottom. Specifically, at a holding time of 1 min the stress corresponds to a high value (509 MPa); at 7 min it drops to a minimum (463 MPa). However, when the holding time is further extended to 9 min, the residual stress rises back to 512 MPa. The top of the diamond is under tensile stress whereas the bottom is under compressive stress, which is consistent with the mechanical response of diamond being squeezed by filler shrinkage during cooling and further verifies that thermal-expansion mismatch is the core source of residual stress.



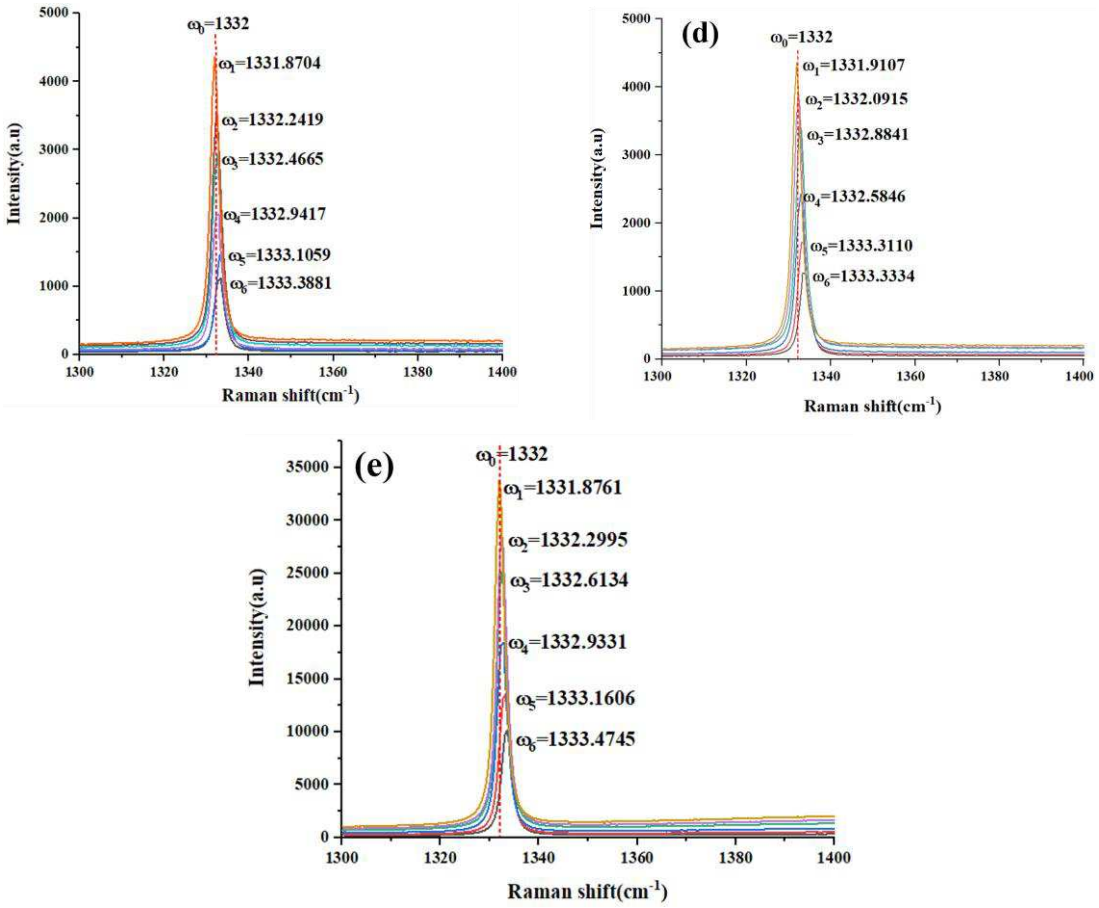


Fig. 6 Raman spectra of diamond particles under different brazing holding times.

3.4 Comparison and verification of simulation with experiments

As can be seen from Fig. 7, the trends and values of the measured values (point F) and the simulated values (the diamond/filler contact region) are in good agreement, indicating that the finite element method can effectively predict the residual stress in brazed diamond. The detailed comparison data and deviation analysis are given in the following discussion.

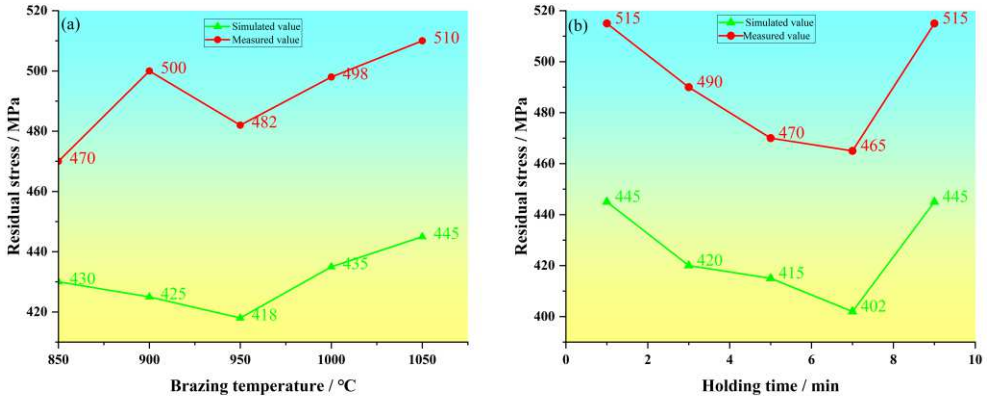


Fig. 7 Comparison between simulated and measured residual stresses: (a) different brazing temperatures; (b) different holding times.

From Fig. 7, the trends and values of the simulated and measured results are close, indicating that the finite element method can effectively predict the residual stress in brazed diamond. Fig. 7(a) shows the comparison at different brazing temperatures: as the temperature increases from 850 to 1050 °C, both simulated and measured values exhibit a nonlinear trend of first decreasing and then increasing, reaching the minimum simultaneously at 950 °C—417.3 MPa (simulated) and 481 MPa (measured). Fig. 7(b) shows the comparison at different holding times (1-9 min): as the holding time increases from 1 to 7 min, the residual stress gradually decreases, reaching the minimum at 7 min (402.1 MPa simulated, 463 MPa measured); when the holding time is further extended to 9 min, the stress rises back to 442.4 MPa (simulated) and 512 MPa (measured). Taken together, Figs. 7(a) and (b) show that 950 °C/7 min is the globally optimal process window for residual stress, which is fully consistent with the foregoing single-variable analysis.

To further quantify the prediction accuracy of the model, the simulated and measured values under each process condition were compared, and the deviation calculation results are shown in Fig. 7. It can be seen that the deviation between the finite element simulated values and the Raman measured values is within 15%, and the variation trend is completely consistent, fully verifying the accuracy and reliability of the finite element model[25,26]. Among them, the deviations at 950 °C and 7 min are the smallest (13.2% and 13.2%, respectively), while those in the low-temperature region (850 and 900 °C) are slightly larger (14.3% and 14.5%). This mainly originates from the fact that, in the actual brazing process,

the arrangement of diamond grits varies and the material properties may change locally due to the actual metallurgical reactions, whereas idealized assumptions were adopted in the model. .

3.5 Grinding tests and wear-morphology analysis

The friction coefficient and the material removal of the workpiece are important indicators for evaluating the wear resistance and cutting efficiency of brazed specimens. A high friction coefficient during grinding indicates a large cutting force on the diamond grits; as grinding time increases, the greater cutting heat and local load will damage the grits, thereby reducing the cutting efficiency and service life of the diamond tool. Therefore, a lower friction coefficient indicates better performance of the diamond tool. Diamond grinding disks prepared by different brazing processes were used to grind SiC wafers; each disk was ground 5 times, each lasting 1 min, and was cleaned with acetone after each grinding before the next. A high-precision friction and wear tester was used to acquire the friction coefficient, and an electronic balance was used to record the weight loss of the SiC wafer after each grinding, as shown in Fig. 8.

In the analysis of the effect of brazing temperature (Fig. 8(a)), the friction coefficient of the 850 °C specimen shows a 'first rise then fall' trend (average friction coefficient 0.25 → 0.28 → 0.23). This is mainly because the holding force of the filler on the diamond grits is low at this temperature, and the grits gradually fall off during grinding (average shedding rate of 80.61%); the friction coefficient then decreases because the filler and steel substrate participate in grinding during the fourth grinding. Since the 850 °C specimen has a high shedding rate, it does not participate in the fifth grinding. Over the four grindings, the SiC weight loss changes as 15 → 13 → 10 → 7 mg. In contrast, the friction coefficients of the 900 and 950 °C specimens generally show a 'first decrease then increase' trend: specifically, at 900 °C the average friction coefficient is 0.313 → 0.297 → 0.302 → 0.28 → 0.30, with corresponding SiC losses of 27 → 28 → 13 → 16 → 14 mg; at 950 °C the average friction coefficient is 0.252 → 0.254 → 0.242 → 0.268 → 0.271, with SiC losses of 36 → 38 → 20 → 35 → 21 mg. In comparison, the high-temperature (1000 and 1050 °C) specimens also generally show a 'first rise then fall' trend: at 1000 °C the average friction coefficient changes as 0.311 → 0.333 → 0.316 → 0.336 → 0.318, with corresponding five-time SiC losses of 32 → 28 → 14 → 26 → 28 mg; at 1050 °C the average friction coefficient changes as 0.288 →

0.391 → 0.294 → 0.315 → 0.268, with corresponding losses of 29 → 21 → 18 → 24 → 19 mg.

The effect of holding time on the friction coefficient is also regular (Fig. 8c). The friction coefficient of the 1-min specimen is extremely unstable, varying as 0.09 → 0.15 → 0.18 → 0.085 → 0.13; it is also accompanied by diamond shedding during grinding, and because of the short holding time the grit exposure is high and the chip space is large, so although the friction coefficient is low the total SiC loss is only 36 mg. The 3-min specimen has an average friction coefficient of 0.273 → 0.242 → 0.237 → 0.308 → 0.155, with corresponding SiC losses of 18 → 10 → 3 → 9 → 5 mg. Compared with 5 min, the 7-min specimen has a lower friction coefficient over the five grindings, at 0.197 → 0.208 → 0.214 → 0.225 → 0.192. The SiC weight-loss data (43 → 34 → 33 → 24 → 25 mg) further verify the correlation between friction coefficient and wear morphology; under this process the total SiC weight loss is the highest (159 mg). As the holding time increases to 9 min, the friction coefficient of the specimen is unstable, varying as 0.278 → 0.294 → 0.282 → 0.192 → 0.278, with corresponding SiC losses of 35 → 28 → 19 → 23 → 18 mg.

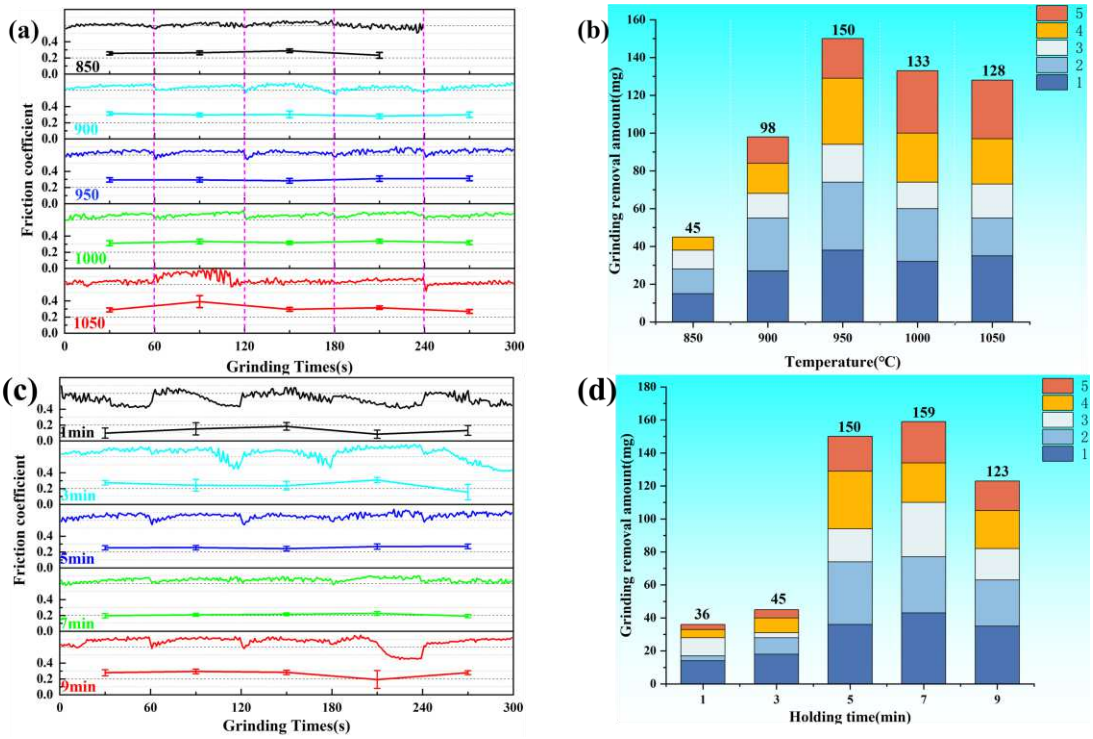


Fig. 8 (a) Friction coefficients and average friction coefficients of diamond grinding disks at different brazing temperatures; (b) SiC weight loss after each grinding at different brazing

temperatures; (c) friction coefficients and average friction coefficients at different holding times; (d) SiC weight loss after each grinding at different holding times.

The morphological statistics in Fig.9 quantify the wear mode distribution of diamond grits at different brazing temperatures. At 850° C, the proportions of shedding and macro-fragmentation were significant, reaching 80.61% and 8.98%, respectively, indicating that insufficient filler metal fluidity at low temperatures led to weak interfacial bonding. When the temperature rose to 900° C, the diamond shedding rate decreased markedly to 2.22%. At 950° C, the proportion of micro-fragmentation surged to 15.54%, while the probability of macro-fragmentation dropped to a minimum of 4.44%, demonstrating that appropriate elevation of brazing temperature effectively reduced diamond residual stress, improved bonding strength, and promoted diamond self-sharpening ability. However, after the temperature reached 1000° C and 1050° C, the macro-fragmentation ratio increased from 11.11% to 13.33%, and the micro-fragmentation ratio increased from 13.33% to 15.56%, which is attributed to the increased interfacial brittleness caused by larger residual stress at high temperatures.

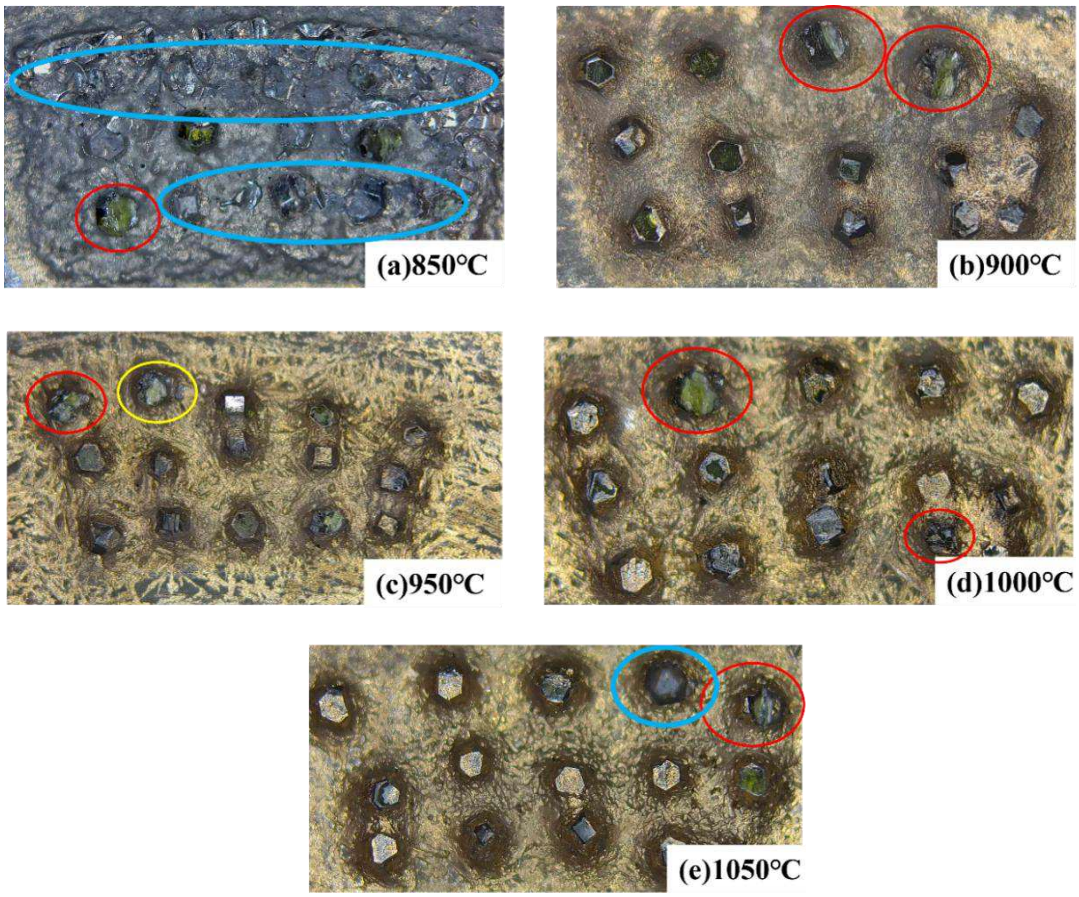


Fig. 9 Statistics of diamond specimens' morphology after grinding at different temperatures

(a) 850℃; (b) 900℃; (c) 950℃; (d) 1000℃; (e) 1050℃

The morphological statistics in Fig. 10 quantify the wear mode distribution of diamond grits at different brazing temperatures, revealing the regulatory effect of temperature on grit failure behavior. As shown in Fig. 10(a), at 850°C, the proportions of shedding and macro-fragmentation were significant, reaching 80.61% and 8.98%, respectively, indicating that insufficient filler metal fluidity at low temperatures led to weak interfacial bonding, causing rapid shedding or fracture of grits due to load transfer failure. When the temperature rose to 900°C, as shown in Fig. 10(b), the diamond shedding rate decreased significantly to 2.22%, indicating a substantial improvement in the holding force of the filler metal on diamond. As shown in Fig. 10(c), when the temperature rose to 950°C, the proportion of micro-fragmentation surged to 15.54%, while the probability of diamond macro-fragmentation dropped to a minimum of 4.44%, indicating that appropriately increasing the brazing temperature effectively reduced diamond residual stress, improved the bonding strength between filler metal and diamond, promoted diamond self-sharpening ability, and effectively maintained cutting efficiency. However, after the temperature reached 1000°C and 1050°C, the diamond macro-fragmentation ratio increased from 11.11% to 13.33%, and the micro-fragmentation ratio increased from 13.33% to 15.56%, as shown in Fig. 10(d-e). This is associated with the increased interfacial brittleness caused by larger residual stress inside the joint at high temperatures, which reduced the bonding strength between filler metal and diamond and deteriorated the service life of diamond

tools.

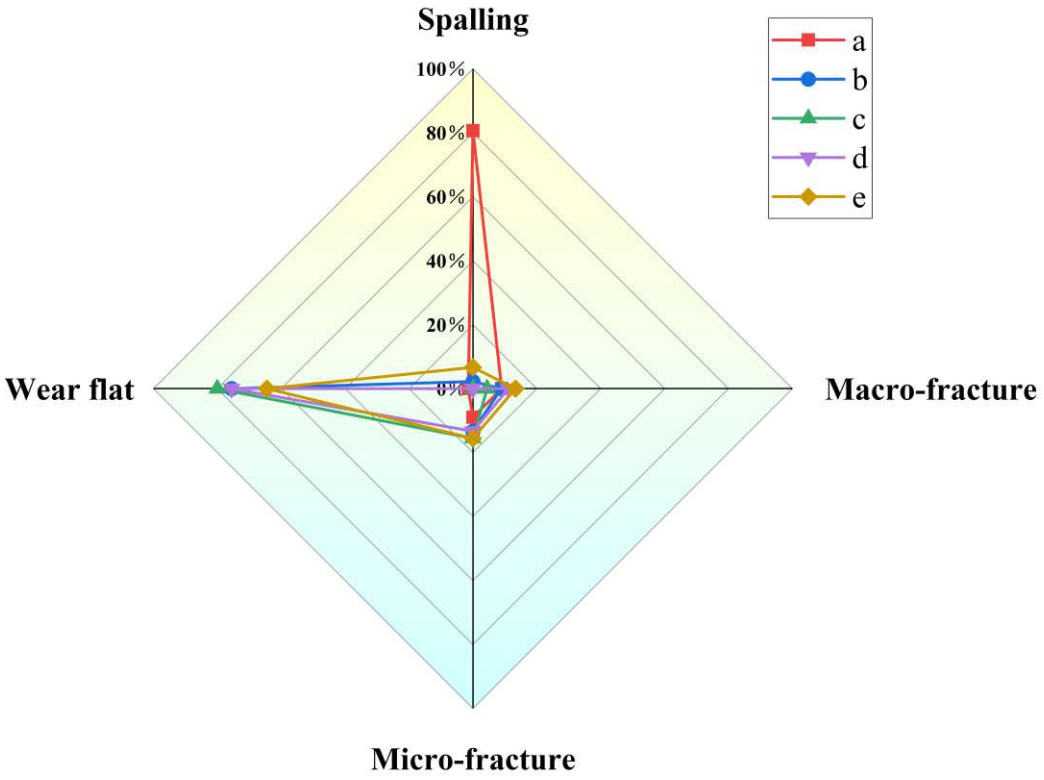


Fig. 10 Statistics of diamond specimens' morphology after grinding at different temperatures: (a) 850 °C, (b) 900 °C, (c) 950 °C, (d) 1000 °C and (e) 1050 °C.

The macroscopic morphology of diamond specimens after grinding under different holding times is shown in Fig. 11. The specimen with a holding time of 1 min exhibited the poorest wear resistance, with partial shedding of diamond particles on the specimen surface after grinding. For the specimen with a holding time of 3 min, cracks and macro-fragmentation were observed on some diamond grits. The specimen with a holding time of 7 min showed smoothing and micro-fragmentation of diamond grits after grinding, which is considered an ideal wear condition because it exposes new sharp edges while maintaining particle volume, thereby preserving the cutting efficiency of the tool. With further increase in holding time, macro-fragmentation of diamond grits reappeared.

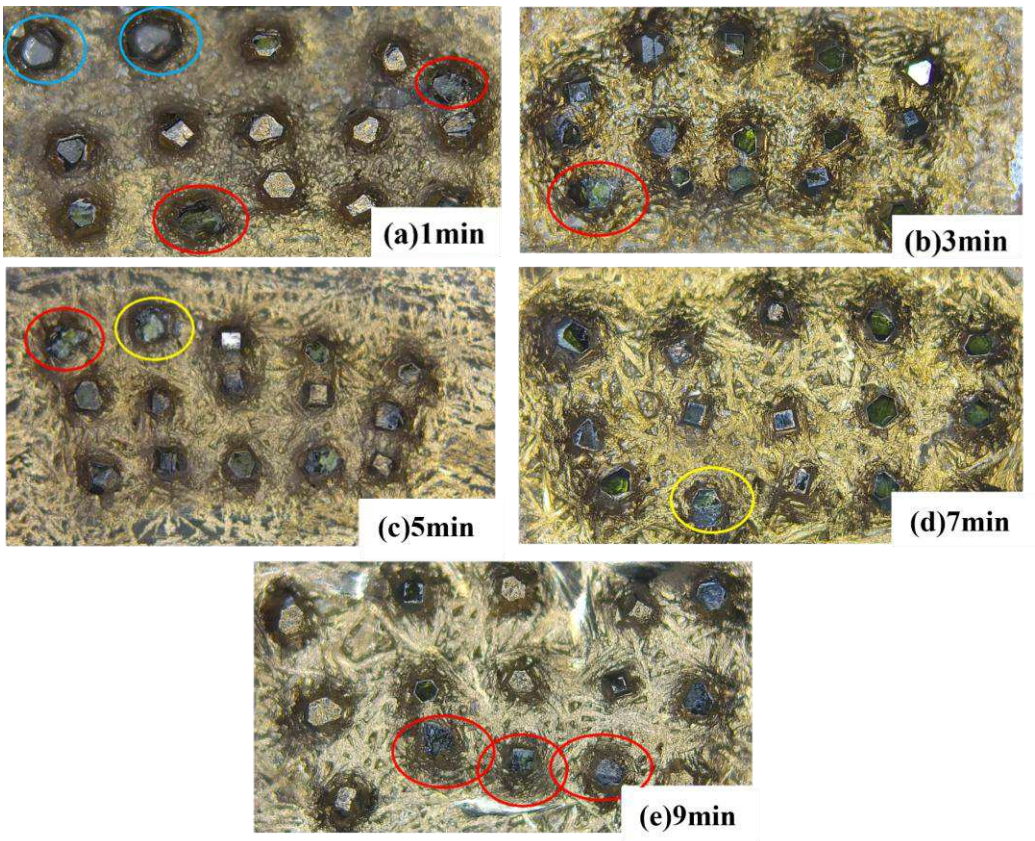


Fig. 11 Macroscopic morphology of diamond specimens after grinding at different holding times

Fig. 12 quantifies the wear mode distribution of diamond grits under different holding times through morphological statistics, revealing the regulatory mechanism of interfacial reaction kinetics on grit failure behavior. At a holding time of 1 min, the proportions of shedding and macro-fragmentation were relatively high at 15.55% and 8.89%, respectively, as shown in Fig. 12(a). This may be attributed to insufficient diffusion of Ti elements in the filler layer, resulting in a discontinuous TiC layer at the interface that weakened the bonding strength, making the grits susceptible to failure under cutting load impact. When the holding time was extended to 3 min, diamond grit shedding no longer occurred, but the proportions of macro-fragmentation and micro-fragmentation were both 11.11%, as shown in Fig. 12(b). As the holding time was further extended to 5 min and 7 min, the micro-fragmentation ratio changed from 15.54% to 6.88%, and the macro-fragmentation ratio decreased from 4.44% to 3.58%. This indicates that at a holding time of 7 min, diamond grits possess both good self-sharpening ability and high bonding strength, mainly attributed to the release of diamond residual stress under this process condition, which effectively improved the service life of diamond tools. However, when the holding time increased to 9 min, the macro-fragmentation ratio rebounded to 17.78%, as shown in Fig. 12(e). This suggests that prolonged holding time

increases the joint residual stress, exacerbating particle fracture under non-coordinated deformation and reducing the service life of grits.

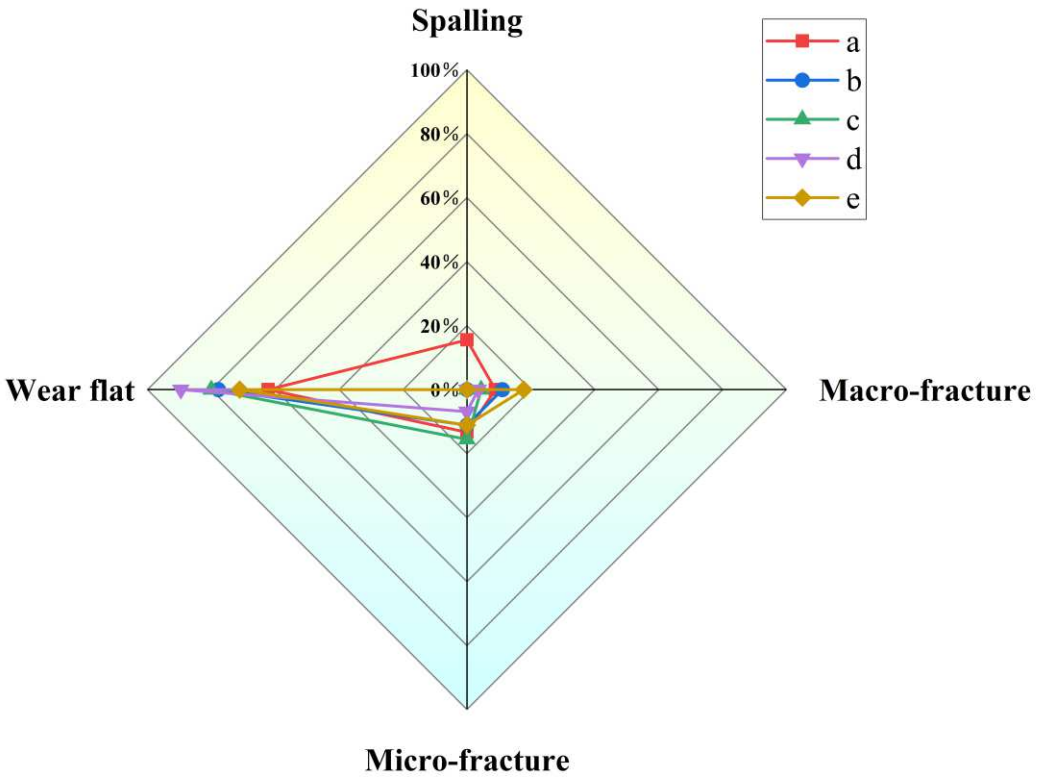


Fig. 12 Statistics of diamond specimens' morphology after grinding under different heat preservation: (a) 1 min, (b) 3 min, (c) 5 min, (d) 7 min and (e) 9 min.

4 Conclusions

(1) The three-dimensional thermo-mechanical coupled finite element model established in this study can accurately predict the residual-stress distribution in Cu-20Sn-10Ti brazed diamond. The simulated values agree well with the Raman measured values, with deviations within 15%, verifying the reliability of the model.

(2) Both brazing temperature and holding time exhibit a nonlinear trend of first decreasing and then increasing. At 950 °C and 7 min the residual stress reaches minimum values of 417.3 MPa and 402.1 MPa (FEM), respectively, or 463 MPa (Raman), and 950 °C/7 min is identified as the optimal process window.

(3) The peak residual stress is always concentrated near the diamond/filler interface and decays rapidly with distance, which is directly related to the thermal-expansion mismatch among diamond, filler and steel matrix.

(4) Grinding tests show that under the 950 °C/7 min process the diamond grits exhibit a moderate micro-fracture ratio, combining good self-sharpening ability with bond strength, and the tool achieves optimal wear resistance. This study provides a scientific basis for the control of residual stress and process optimization of brazed diamond tools.

Data availability

Data will be made available on request.

Key Science and Technology Project of Henan Province(Project No.262102221025, 262102230126）

Key Scientific Research Projects of Colleges and Universities in Henan Province (No. 27AQ430004)

References

[1] Field J E. The Properties of Natural and Synthetic Diamond. London: Academic Press; 1992.

[2] Malkin S, Guo C. Grinding Technology: Theory and Applications of Machining with Abrasives. 2nd ed. New York: Industrial Press; 2008.

[3] Tönshoff H K, Friemuth T, Becker J C. Process monitoring in grinding. CIRP Annals 2002;51(2):551–71.

[4] Wu C, Fang J, Chen X, et al. Comparative study on preparation and performance of electroplated and brazed diamond tools. Diamond and Related Materials 2018;84:151 – 8.

[5] Huang S, Tsai H, Lin C. The characteristics of brazed diamond tools. International Journal of Refractory Metals and Hard Materials 2015;48:95 – 103.

[6] Chattopadhyay A K, Hintermann H E, Chollet L. On the morphology of brazed diamond grits. Surface and Coatings Technology 1991;45(1 – 3):293 – 8.

[7] Sung C M, Tai M F. Whiskers and rocks: a model of low-pressure diamond growth. Diamond and Related Materials 1994;3(7):929 – 44.

[8] Liu H, Yang H, Shen B, et al. Interfacial microstructure and mechanical properties of diamond/Cu – Sn – Ti composite brazed joints. Materials & Design 2016;90:524 – 31.

[9] Khalid F A, Beffort O, Klotz U E, et al. Microstructure and interfacial characteristics of brazed diamond joints. Diamond and Related Materials 2004;13(10):1887 – 92.

[10] Liang Z, Wang X, Wu Y, et al. Development and application of ultra-precision grinding technology. Chinese Journal of Mechanical Engineering 2020;33(1):1 – 15.

[11] Akaishi M, Yamaoka S, Tanaka J, et al. Thermoelastic stress analysis in diamond/metal composites. Journal of Materials Science 1995;30(23):6065 – 70.

[12] Bar-Cohen Y, Mal A K, Meng C H, et al. Residual stresses in brazed joints. Journal of Engineering Materials and Technology 1998;120(2):125 – 30.

[13] Pan R, Wang J, Li W, et al. Effect of residual stress on the fracture of brazed diamond. Surface and Coatings Technology 2014;248:59 – 66.

[14] Liu Y, Huang H, Xu X, et al. Finite element analysis of residual stress in diamond grinding tools. Materials 2019;12(18):2950.

[15] Ferrari A C, Robertson J. Interpretation of Raman spectra of disordered and amorphous carbon. Physical Review B 2000;61(20):14095 – 107.

[16] Prawer S, Nemanich R J. Raman spectroscopy of diamond and doped diamond. Philosophical Transactions of the Royal Society A 2004;362(1824):2537 – 65.

[17] Chandrasekar S, Farris T N, Licht R H, et al. Finite element simulation of brazing process. Journal of Materials Processing Technology 2005;167(1):140 – 9.

[18] Zhang F, Chen Y, Fu Y. Finite element and Raman analysis of residual stress in brazed diamond grits. Surface Engineering 2015;31(5):340 – 7.

[19] Akbari M, Buhl S, Leinenbach C, Spolenak R, Wegener K. Thermomechanical analysis of residual stresses in brazed diamond metal joints using Raman spectroscopy and finite element simulation. Mechanics of Materials 2012;52:69 – 77.

[20] Buhl S, Leinenbach C, Spolenak R, Wegener K. Microstructure, residual stresses and shear strength of diamond – steel joints brazed with a Cu – Sn-based active filler alloy. International Journal of Refractory Metals and Hard Materials 2012;31:38 – 44.

[21] Li J, Zhang H, Liu Y, et al. 3D FEM and experimental verification of residual stress in Ni–Cr brazed diamond. International Journal of Refractory Metals and Hard Materials 2020;88:105197.

[22] Xia G Z. Practical Handbook of Engineering Materials. Beijing: China Standards Press; 1989. [In Chinese.]

[23] China Abrasives & Abrasives Industry Corporation. Technical Handbook of Abrasives and Grinding Tools. Beijing: Weapons Industry Press; 1993. [In Chinese.]

[24] Yan J Y. Finite element simulation and experimental study on thermal stress of brazed diamond grit joints [Master’s thesis]. Xiangtan: Hunan University of Science and Technology; 2015. [In Chinese.]

[25] Sung C M. Brazed diamond grid: a revolutionary new grinding wheel. Diamond and Related Materials 1999;8(1):154–61.

[26] Yokota H, Okada M, Watanabe T, et al. Thermal stress analysis of diamond tools by FEM. Journal of Materials Processing Technology 2003;138(1–3):614–8.